Electrochemical characterization of para- and meta- nitro substituents in aqueous media of new antichagasic pharmaceutical leaders

Caroline G. Sanz , Kevin A. Dias , Raphael P. Bacil , Ricardo A.M. Serafim , Leandro H. Andrade , Elizabeth I. Ferreira , Silvia H.P. Serrano

PII: S0013-4686(20)31975-7
DOI: https://doi.org/10.1016/j.electacta.2020.137582
Reference: EA 137582

To appear in: *Electrochimica Acta*

Received date: 5 August 2020
Revised date: 12 November 2020
Accepted date: 28 November 2020

Please cite this article as: Caroline G. Sanz , Kevin A. Dias , Raphael P. Bacil , Ricardo A.M. Serafim , Leandro H. Andrade , Elizabeth I. Ferreira , Silvia H.P. Serrano , Electrochemical characterization of para- and meta- nitro substituents in aqueous media of new antichagasic pharmaceutical leaders, *Electrochimica Acta* (2020), doi: https://doi.org/10.1016/j.electacta.2020.137582

Highlights

- Electrochemical characterization of these two synthesized antichagasic leaders was performed in aqueous media using cyclic, differential, and square wave voltammetry
- Mesomeric correlation towards the electrochemical stabilization of the nitro radical anion was addressed using electronic flux of both radicals formed
- Interaction with oxygen and cysteine further confirmed the electrochemical detection of the nitro radical anion and other reactive intermediates

Electrochemical characterization of *para*- and *meta*- nitro substituents in aqueous media of new antichagasic pharmaceutical leaders

Caroline G. Sanz[a], Kevin A. Dias[a], Raphael P. Bacil[a], Ricardo A.M. Serafim[b], Leandro H. Andrade[a], Elizabeth I. Ferreira[b], Silvia H. P. Serrano[a]*

[a] Department of Fundamental Chemistry, Institute of Chemistry, University of São Paulo, 05508-000 São Paulo/SP, Brazil

[b] Department of Pharmacy, Faculty of Pharmaceutical Sciences, University of São Paulo, 05508-900 São Paulo/SP, Brazil.

*Corresponding Author
Tel: +551130912687
e-mail: shps@iq.usp.br

Abstract

The electrochemical reduction mechanism of two isomers of position drug leaders against Chagas disease, *p*-nitrosulfonylhydrazine derivative (*p*-NSF), and *m*-nitrosulfonylhydrazine derivative (*m*-NSF), was investigated in aqueous media and in the absence of oxygen using voltammetric techniques. The main reduction process was attributed to the reduction of the nitro group (E_{pc} (*p*-NSF) = -0.58 V and E_{pc} (*m*-NSF) = -0.62 V), generating nitroso derivative in intermediate and higher values of pH and hydroxylamine in lower values of pH. Another reduction process in a less negative potential value was only observed for *p*-NSF and attributed to the generation of the nitro radical anion. The difference in the reduction potentials between both compounds and the presence of another reduction process for *p*-NSF was associated with the position of the nitro group, due to the distinct stabilization of the reduction intermediates by the aromatic ring. A catalytic response for the reduction process of the nitro anion radical was observed for *p*-NSF in the presence of oxygen, given that its magnitude of current increased when increasing the oxygen availability. Also, for *m*-NSF, this reduction process could be detected, even though it was not observed in the voltammograms in the absence of oxygen. This further confirmed the generation of the nitro radical anion, since it reacts with molecular oxygen and regenerates the initial nitro compound. The interaction with cysteine was also evaluated, which favored the reduction process towards the generation of the nitroso derivative due to adduct formation, destabilizing the reduction process regarding the nitro radical anion. Therefore, electrochemical experiments can evaluate how different isomers of position and other coupled functional groups affect the reduction of the nitro group and, consequently aid in the design of new classes of antichagasic pharmaceuticals, with improved stability of reactive intermediates that are often correlated with the degree of injury towards the parasite.

Keywords: Chagas disease; nitro compounds; electrochemical characterization; nitro anion radical; voltammetry

1. INTRODUCTION

Neglected diseases, by definition, are those caused by parasites or infectious agents, and considered endemic in underdeveloped and developing countries where there is a lack of interest in the optimization of drugs towards treatment, prevention, cure, or even their diagnosis [1,2]. These fall into a comprehensive group of endemics that remains a neglected target in research regarding new drug development, where only 1.15% of new drugs, registered between 1975 and 2004, were intended for its control, even though the global health burden surpasses 10% of all disease occurrence [3–5]. Chagas disease, a parasitic tropical disease of the American continent, caused by the protozoan *Trypanosoma cruzi*, and discovered by Carlos Chagas in 1909, belongs to this neglected endemic group [6,7]. The mechanism of transmission of the parasite is primarily through a mechanical vector, nocturnal insects of the *Triatominae* family [8], which mainly affects low-income populations susceptible to poor sanitation conditions, and induces characteristic symptoms that may take up to 30 years to manifest [9]. The rate of morbidity and mortality is significant, given that the disease entails a chronic evolutionary heart condition, victimizing up to 20% or more of infected individuals [10].

Trypanocidal drugs such as benznidazole and nifurtimox, introduced in 1971 and 1965, respectively, were and still are used to treat Chagas disease, acting mainly by inhibiting enzymes necessary to the defense mechanism of the parasite cells, however also cytotoxically affecting the individual [11]. Although effective, the use of these drugs is linked in 40% of cases to side effects such as skin diseases, brain toxicity, and digestive system irritation [12,13].

One of the routes in the development of drugs with antichagasic activity is based on their ability to affect the *Trypanosoma cruzi* detoxification mechanism, making it

deficient to combat oxidative stress of the cell. The parasite mechanism of defense is sustained by a specific enzyme called trypanothione reductase (TR), given that it lacks the enzymes catalase, glutathione peroxidase, and glutathione reductase, responsible for a significant portion of oxidative control in mammals [14]. Certain antichagasic drugs act indirectly to inhibit TR, making it difficult to reduce trypanothione disulfide (physiological substrate of the enzyme) to its thiol component, which in turn is responsible for the control of oxidative stress [15]. Therefore, inhibiting the action of the enzyme increases the parasite's vulnerability to the drug, causing its death through the increase in the concentration of reactive oxygen species in the intracellular environment [15,16].

Both benznidazole and nifurtimox are part of an antichagasic class of drugs that presents a nitro ($-NO_2$) functional group usually linked to aromatic rings. Its cytotoxicity is associated with the formation and stabilization of the anionic nitro radical ($R\text{-}NO_2^{\bullet -}$), in which the reduction potential corresponding to the redox pair $R\text{-}NO_2/R\text{-}NO_2^{\bullet -}$ is usually an indicator of drug efficiency [17]. The anionic nitro radical and its derivatives (RNO, nitrous derivative and RNHOH, hydroxylamine) can interact toxically in two ways: acting directly to interfere with the parasite's oxygen metabolism, or interacting directly with DNA by destabilizing the double helix through reactions with nitrogenous bases (depending on pH, specifically thymine and adenine), besides additionally affecting lipids and proteins in a less significant way [18]. The stability of the nitro compound reduction intermediates is related to the degree of injury it may promote to biomolecules, or else, the slower the rate of decomposition of the nitro radical anion and the easier it is to be generated (both correlated to its reduction potential), the larger and faster will be the damage caused [19]. The bioactive compound crosses the cell membrane by passive diffusion, and its concentration in the

intracellular environment increases while reactive species, coming from the bioreduction of these nitro compounds destabilize the membrane, Figure 1.

FIGURE 1

Electrochemical measurements have been used to correlate the mechanism of action of drugs with their redox potential and biological efficiency in biomedical applications, however, one must address the complexity of these systems regarding stereochemistry, diffusion, solubility, and membrane permeability, amongst others [20]. Still, given that most important physiological processes occur through charge transfer reactions, potentially induced heterogeneous processes in aqueous or organic media can be used to clarify redox processes and reactive intermediate stabilization. Linear and pulse voltammetry are often used to elucidate the biological process of interest without the necessity of spectroscopic and/ or chromatographic methods and gather further evidence towards biological electron-transfer reactions [21].

A variety of aromatic nitro compounds has been electrochemically characterized, such as nitrofuran [22–25] and nitroimidazole derivatives [26–29]. Still, mostly all experiments were performed in aprotic or organic media, to further aid in the stabilization of intermediate radicals [30,31] and access the reduction potential of pharmaceutical compounds and mechanism of action. The reduction processes were also evaluated at different electrode materials, such as mercury [32], carbon [33], boron-doped diamond [34,35], and modified electrodes [36], in which the properties of the transducer material improved the stabilization of reactive intermediates. Still, the main interest regarding the electrochemical study of this class of compounds are either biological [37–40] or their potential damage to DNA [28,41–48].

The molecular design of isomers of position in ring systems of compounds containing sulfonylhydrazone scaffold can be used as a strategy to generate new antichagasic leaders since the presence of the nitro functional group ($R\text{-}NO_2$) in the benzene ring at the *para*- and *meta*- positions promotes, in the intracellular environment, major reactivity of the intermediates from the nitro bioreduction process. According to a previous study with acylhydrazone derivatives, its bioisostere sulfonylhydrazone group may also act directly on the active site of cruzain, an endoprotease vital to the parasite's nutrition, consequently increasing the selectivity in comparison to the current benznidazole treatment [49]. Also, the presence of nitric oxide in the intracellular environment aids the rupture of the plasma membrane of the etiological agent, although its excessive release may also damage the host cells. Nitric oxide release occurs in neutral and alkaline medium, in which the furoxan ring from both leaders undergoes hydrolysis [50].

Therefore, the objective of this work was to describe the synthesis procedure and electrochemical reduction mechanisms of two pharmaceutical leaders against Chagas disease: (2-Oxide of *(E)*-3-methyl-4-((2-((*para*-nitrophenyl)sulfonyl)hydrazone)methyl) -1,2,5-oxadiazole) and (2-Oxide of *(E)*-3-methyl-4-((2-((*meta*-nitrophenyl)sulfonyl) hydrazone)methyl)-1,2,5-oxadiazole), denominated *p*-NSF and *m*-NSF, respectively. The stabilization of the nitro radical anion from the reduction processes of the nitro group was evaluated in aqueous media at bare glassy carbon electrode in the absence and the presence of oxygen. Given that compounds containing thiol groups on their structure can form adducts with one of the intermediates from the nitro group reduction process, this interaction was evaluated. Their redox potentials and intermediate stabilization were used to establish the degree of injury between both leaders and compared with similar compounds that present the nitro

group at the same position and that were already tested *in vitro* against the protozoan [49].

2. EXPERIMENTAL

2.1 Reagents

Britton-Robinson (BR) buffer 0.04 M was prepared by dissolving the appropriate amount of sodium borate and diluting the appropriate volume of phosphoric acid and acetic acid in deionized water. The pH adjustment was made with small volume additions of 6.0 M sodium hydroxide solution in a pH range between 4.0 and 10. All reagents employed were of analytical grade and obtained from Merck, Rio de Janeiro, Brazil. Nitrogen and oxygen gases used in the experiments were of R grade and purchased from Air Products, São Paulo, Brazil. All buffer solutions were prepared using Millipore Direct-Q ultrapure water with resistivity ≥ 18 MΩ cm. For the synthetic section of this work, reagents and solvents were purchased from commercial suppliers and used as received.

2.2 Instrumentation

Buffer solution's pH measurements were performed with pH-meter model 654 and a combined glass electrode (Ecotrode Plus, model 60262100, Metrohm). Electrochemical measurements were performed using a computer-controlled μ-Autolab Type III potentiostat-galvanostat running with software NOVA for Windows version 1.11. For the organic synthesis of *p*-NSF and *m*-NSF, the progress of all reactions was monitored by analytical thin-layer chromatography, which was performed on silica-gel 60 GF (5-40 μM thickness) plates. Visualization was accomplished with UV light. Melting points were measured with an electrothermal melting-point apparatus (Büchi, M-565 model) in open capillary tubes and are uncorrected. ^{1}H and proton decoupled ^{13}C NMR spectra were scanned on Bruker AVANCE™ NMR spectrometer in DMSO-d_6 at

300 MHz (^{1}H) and 75 MHz (^{13}C). The chemical shifts (δ) are reported in ppm. High-resolution mass spectrometry (HRMS) was performed using electrospray ionization (ESI). The parent ions ([M - H^+]) or ([M + Na^+]) are quoted.

2.3 Intermediates (*p*-NS, *m*-NS and *p*-MS) and Antichagasic Leaders (*p*-NSF and *m*-NSF) Synthesis

A straightforward convergent synthetic pathway was chosen for *p*-NSF and *m*-NSF synthesis (Scheme 1). In the superior branch, the sulfonyl hydrazides intermediates *p*-NS, *m*-NS, and *p*-MS was achieved by treating the correspondent sulfonyl chlorides (1a-c) with hydrazine hydrate (step *a*). Concerning the lower branch, the 3-methyl-4-furoxancarbaldehyde (3) was obtained by the reaction between crotonaldehyde (2) and aqueous sodium nitrite in the presence of acetic acid, following the methodology described by Fruttero *et al.* [51]. Finally, in the convergent step, the sulfonyl hydrazones *p*-NSF and *m*-NSF were obtained by the acid-mediated condensation of *p*-NS and *m*-NS with 3, respectively. The purity of all target compounds was found to be >95%.

SCHEME 1

2.3.1 Procedure '*a*': synthesis of sulfonyl hydrazides (Scheme 1; intermediates *p*-NS, *m*-NS, and *p*-MS)

The respective sulfonyl chloride (1a-c) (10 mmol) was added slowly in a solution of hydrazine hydrate 80% (25 mmol) and THF (4 mL) over stirring at 0 °C. After the total consumption of the starting material, water was added and the resulting solid was filtered and washed with cold water to obtain the respective pure sulfonyl hydrazides.

2.3.1.1 *p*-Nitrobenzenesulfonylhydrazide (*p*-NS)

Pale yellow solid; Yield 91%. **^{1}H NMR** (300 MHz, DMSO-d_6), **δ** (ppm)**:** 8.43 (d, *J* = 9.0 Hz, 2H), 8.13 (d, *J* = 9.0 Hz, 2H), 7.96 (s, 1H), 3.45 (s, 2H).

2.3.1.2 *m*-Nitrobenzenesulfonylhydrazide (*m*-NS)

White solid; Yield 88%. **^{1}H NMR** (300 MHz, DMSO-d_6), **δ** (ppm)**:** 8.75 (bs, 1H), 8.54-8.48 (m, 2H), 8.20 (ddd, *J* = 7.8 Hz, *J* = 2.4 Hz, *J* = 0.6 Hz, 1H), 7.91 (dt, *J* = 7.8 Hz, *J* = 0.6 Hz, 1H), 4.34 (bs, 2H).

2.3.1.3 *p*-Methylbenzenesulfonylhydrazide (*p*-MS)

Colourless crystals; Yield 89%. **^{1}H NMR** (300 MHz, DMSO-d_6), **δ** (ppm)**:** 8.20 (s, 1H), 8.43 (d, *J* = 8.1 Hz, 2H), 8.13 (d, *J* = 8.1 Hz, 2H), 4.00 (bs, 2H).

2.3.2 Procedure '*b*': synthesis of 3-methyl-4-furoxancarbaldehyde (Scheme 1, intermediate 3)

Compound 3 was synthesized from 2 according to the methodology previously described by Fruttero *et al.* [51].

2.3.3 Procedure '*c*': synthesis of sulfonyl hydrazones (Scheme 1, final compounds *p*-NSF and *m*-NSF)

The synthesis of *p*-NSF and *m*-NSF has already been described [50]. The intermediate 3 (2 mmol) was reacted with the corresponding sulfonyl hydrazides (*p*-NS, *m*-NS) (2 mmol) using acid catalysis (0.1 mL of concentrated HCl) in anhydrous methanol (50 mL) as a solvent. The reaction was kept stirring under reflux until the total consumption of the starting materials. After cooling to room temperature, cold water was added, and the resulting solid was filtered and washed with cold water to obtain the pure final product.

2.3.3.1 (*E*)-3-methyl-4-((2-((4-nitrophenyl)sulfonyl)hydrazono)methyl)-1,2,5-oxadia-zole 2-oxide (*p*-NSF)

Pale yellow solid; Yield 87%; **m.p.:** 160-162 °C. **^{1}H NMR** (300 MHz, DMSO-d_6), **δ** (ppm)**:** 8.45 (d, *J* = 8.7 Hz, 2H), 8.11 (d, *J* = 8.7 Hz, 2H), 7.98 (s, 1H), 2.19 (s,

3H). **^{13}C NMR** (75 MHz, DMSO-d_6), **δ** (ppm)**:**153.0, 150.1, 143.5, 136.4, 128.8, 124.7, 111.2, 9.0. **HRMS** (ES-, TOF-MS)**:** calculated for $C_{10}H_9N_5O_6S$ [M - H+]: 326.0195; found: 326.0206.

2.3.3.2 (*E*)-3-methyl-4-((2-((3-nitrophenyl)sulfonyl)hydrazono)methyl)-1,2,5-oxadia-zole 2-oxide (*m*-NSF)

Pale yellow solid; Yield 91%; **m.p.:** 167-169 °C. **^{1}H NMR** (300 MHz, DMSO-d_6), **δ** (ppm)**:** 8.54 (d, 2H), 8.28 (d, *J* = 8.7 Hz, 1H), 7.95 (t, *J* = 8.7 Hz, 2H), 2.18 (s, 3H). **^{13}C NMR** (75 MHz, DMSO-d_6), **δ** (ppm)**:** 153.0, 147.9, 139.5, 136.7, 133.1, 131.6, 128.1, 122.0, 111.2, 8.9. **HRMS** (ES+, TOF-MS)**:** calculated for $C_{10}H_9N_5O_6S$ [M + Na+]: 350.0171; found: 350.0180.

2.4 Electrode Surface Cleaning Procedure

The bare glassy carbon electrode (GCE) surface was polished with a diamond spray down to 1.0 μm particle size from Kemet, United Kingdom, and rinsed thoroughly with deionized water and ethanol. Cyclic voltammograms were recorded in 0.04 M BR buffer pH 7.0, in a potential range from 0.0 V to 1.0 V and scan rate of 100 mV s^{-1} for 5 cycles, to stabilize the baseline.

2.5 Electrochemical measurements

All electrochemical measurements were conducted on a one-compartment 10 mL electrochemical cell containing a 1.5 mm diameter (geometric area 0.071 cm^2) glassy carbon electrode (GCE), platinum wire, and Ag/AgCl (saturated KCl) as a working, auxiliary, and reference electrodes, respectively. The experiments were performed at room temperature (25 ± 1 ºC) and, to simulate anaerobic conditions, nitrogen gas was purged in the solution with a flow rate of 0.5 L/min for 15 min before performing the electrochemical measurements. The electrolyte was indicated as predominantly aqueous

(95% aqueous and 5% organic) due to the presence of DMSO from the stock solution of the compounds. The following experimental conditions were used to perform the cyclic voltammetry measurements: E_i = 0.0 V, $E_{\lambda 1}$ = -1.4 V, $E_{\lambda 2}$ = 1.0 V and E_f = 0.0 V, scan rate of 100 mV s^{-1}, step potential of 3 mV, recording 3 cycles in each analysis, unless indicated otherwise. Differential pulse voltammetry measurements were performed using the following experimental conditions: E_i = 0.0 V, E_f = -1.4 V, pulse amplitude of 25 mV, step potential of 2.5 mV, the interval time of 0.5 s, resulting in a scan rate of 5 mV s^{-1}. Square wave voltammetry measurements were performed using the following experimental conditions: E_i = 0.0 V, E_f = -1.4 V pulse amplitude of 25 mV, step potential of 3 mV, frequency of 33 Hz, resulting in a scan rate of 100 mV s^{-1}. The influence of oxygen and cysteine on the electrochemical profile of *p*-NSF and *m*-NSF was evaluated as follows: oxygen was bubbled for 10, 20, and 30s in the electrochemical cell before each measurement; cysteine was added to the electrochemical cell in 1:2, 1:1, and 2:1 molarity ratio cysteine:*p*-NSF (increasing concentration of 0.25 mM, 0.50 mM, and 1.0 mM of cysteine and fixed concentration of 0.50 mM of *p*-NSF).

3. RESULTS AND DISCUSSION

3.1 Voltammetric Characterization

To obtain an overview of the electrochemical profile of the *m*-NSF and *p*-NSF antichagasic leaders, cyclic voltammograms were obtained at GCE in 0.04 M BR buffer pH 7.0 containing 1.0 mM of each compound and in the absence of O_2, Figure 2A and 2B.

FIGURE 2

As can be seen from Figure 2A and 2B, both compounds presented the same number of reduction and oxidation processes, most likely due to the structural similarity

between them. To elucidate and distinguish the nitro group reduction processes from others that might interfere or overlap with them, a comparison with two structurally similar compounds was performed.

In the direct potential sweep, which primarily runs towards negative potential values, the main reduction process can be observed for both compounds, process **2c**, E_{p2c} (*p*-NSF) = -0.62 V and E_{p2c} (*m*-NSF) = -0.64 V. Process **2c** was also observed in a solution containing 1.0 mM of nitrobenzene, which indicates that it corresponds to the main reduction of the nitro group attached to the benzene ring, Figure 2C. This process is usually registered for other nitro compounds in aqueous media, but at peak potentials around -0.40 V to -0.70 V. The change in the peak potential values is usually associated with the position of the nitro group and the aromatic structure attached to it (often a furan or imidazole ring), which are responsible for the stability of the reduction products [30]. Also, the transducer material can split an electrochemical process into two or more components and, in this case, changes in the reduction or oxidation peak potentials for each intermediate can be noticed. Commonly, the electrochemical characterization of these nitro compounds is conducted at carbon-based electrodes (glassy carbon electrodes, boron-doped diamond electrodes, carbon paste electrodes) given their chemical compatibility with aromatic structures.

For both compounds (*p*-NSF and *m*-NSF), changes in the peak potentials and depletion of the magnitude of current were observed for all processes, in the second cycle, most likely due to adsorption of reduction products on the electrode surface.

Process **2a** appears on the cyclic voltammograms for *p*-NSF and *m*-NSF, however, it does not appear at the measurements conducted in the presence of nitrobenzene, which suggests that this oxidation process is unrelated with the nitro group present in the benzene ring, in either *meta*- or *para*- position. Cyclic

voltammograms obtained at GCE in 0.04 M BR buffer solutions, pH 7.0, containing 1.0 mM of *p*-MS, Figure 2D, also present the process **2a**. Given the absence of the sulphonylhydrazide moiety in nitrobenzene, and presence in *p*-NSF, *m*-NSF, and *p*-MS, process **2a** can be associated with the oxidation of the nitrogen close to the sulfone moiety. The oxidation peak potential for process **2a** is similar to other compounds that share this functional group [52].

According to the reduction mechanism for the nitro group in the *p*-NSF and *m*-NSF, it was expected that its free radical reactive intermediate could not be distinctly observed due to their short lifetime in an aqueous medium. Besides, in the cyclic voltammograms obtained for *p*-NSF, another reduction process is present, process **1c**, which does not appear on the voltammograms obtained with *m*-NSF. The peak potential of process **1c** and its absence on the measurements obtained for *m*-NSF indicates that this might be related to one of the reactive intermediates, therefore, the voltammograms obtained on the negative potential region were chosen as the focus of this study.

Besides cyclic voltammetry, relevant results can be also obtained by differential pulse and square wave voltammetry since both techniques present major sensitivity than the cyclic voltammetry. The first one, performed at a slow scan rate, gives an estimative of the number of electrons involved in each electrochemical process, an important step to understanding electron transfer reaction mechanisms, while the last one allows evaluation of the reversibility of the processes at faster scan rates without losing sensitivity.

Differential pulse voltammograms were obtained in 1.0 mM *p*-NSF (BR buffer solution) at GCE in the pH range from 4.0 to 10 in the absence of oxygen. Figure 3A, 3B and 3C shows DP voltammograms in pH 4.0, 7.0 and 10, respectively. The reduction process **3c** only occurs at higher pH values (pH > 8.0) and process **4c** only occurs at

lower pH values (pH < 7.0). However, process **2c** occurs in a wide range of pH values, although at higher pH only one shoulder can be detected (process **1c**). Figure 3D shows the E_p vs. pH plots, and in which is possible to observe that only the processes E_{p2c} and E_{p4c} are pH-dependent.

FIGURE 3

In lower pH values (4.0 < pH < 6.0), E_{p2c} shifts towards more negative values as the pH value increases, according to *(equation 1)*,

E_{p2c} (*p*-NSF) / mV = -0.185 - 0.065 pH (R^2 = 0.991) *(equation 1)*

in which the slope of the curve (close to the theoretical value of 59 mV/pH) indicates that the number of protons and electrons involved in this process is the same. In pH values higher than 6.0, the shift in peak potential no longer occurs, and possibly a different reduction product is formed, and the redox reaction no longer involves protons. At pH ≥ 6.0, a reduction shoulder at E_{p1c} becomes more distinctive. The peak potential for this process remains constant and indicates that this electrochemical step also does not involve protons, as well as process **4c** at higher pH values (pH > 7.0). However, in lower values of pH (4.0 < pH < 7.0), E_{p4c} shifts to a less negative potential when the pH value decreases according to equation *(equation 2)*, showing that the reduction process is facilitated in acidic media.

E_{p4c} (*p*-NSF) / mV = -0.890 -0.055 pH (R^2 = 0.990) *(equation 2)*

The slope of the curve also indicates that the number of protons and electrons involved in this step is the same, similar to that observed in lower pH values for process **2c**. Process **3c** does not suffer any change in the peak potentials in the wide range of pH studied.

The values for $W_{1/2}$ obtained from the DP voltammograms in 0.04 M BR buffer pH 7.0 are -72 and -96 for processes **1c** and **2c**, respectively. Within the margin of error, these values indicate that this reduction processes occur with the transfer of one electron, which is equivalent to 90 mV per electron transferred [53]. Process **3c** and **4c** presented a higher $W_{1/2}$ value, in which more than one electrochemical reduction processes might be overlapped.

At the second DP measurements (data not shown), depletion in the current levels was not observed, which differs from the second cycle registered at the cyclic voltammograms from Figure 2A and 2B. There are two reasons for this difference. Cyclic voltammetry was carried out at 100 mV s^{-1}, therefore, in the second reduction cycle, the sweep is fast enough, that it prevents the electrode surface from being completely renewed with nitro compound, which must arrive by diffusion from within the solution. Also, cyclic voltammograms were obtained after reversing the potential from the positive potential region, where the generated electrochemical oxidation products could be adsorbed on the electrode surface. Differential pulse voltammetry, on the other hand, was carried out at a speed of 5 mV s^{-1}, which infers that a higher amount of time takes place between measurements and, at the second cycle, the surface has been renewed. In this case, given that the DP voltammograms were conducted only in the negative potential sweep, the generated electrochemical products in the first measurement do not interfere with charge transfer for the subsequent measurements.

DP voltammograms were also obtained at GCE in 0.04 M BR buffer, containing 1.0 mM *m*-NSF in a range from pH 4.0 to 10 and in the absence of oxygen. Figure 4A-C, shows DP voltammograms in pH 4.0, 7.0, and 10, respectively.

FIGURE 4

The main processes (**2c** and **4c**) observed for *p*-NSF were present, however, process **1c** did not appear even at pH > 6.0. Process **3c** was only detected in lower pH than those observed with *p*-NSF, even though it is detected at intermediate and higher pH values (pH > 7.0).

The E_p vs. pH plot, Figure 4D, indicates a similarity regarding the reduction processes that the molecules share, **2c**, **3c,** and **4c**. Processes **2c** and **4c** suffer a shift in peak potentials according to *(equation 3)* and *(equation 4)*, as also observed for the *p*-NSF.

E_{p2c} (*m*-NSF) / mV = -0.2890 - 0.056 pH (R^2 = 0.945) *(equation 3)*

E_{p4c} (*m*-NSF) / mV = -0.8438 - 0.065 pH (R^2 = 0.985) *(equation 4)*

Thus, the conclusions about the involvement of protons and electrons are the same already discussed for the *p*-NSF. Process **3c** does not suffer any change in peak potentials, similar as observed at the DP voltammograms obtained with *p*-NSF. The estimative of the number of electrons involved in the reductions process was not performed given that $W_{1/2}$ values indicated that process **3c** can contain more than one reduction process overlapped.

If Figures 3B and 4B are compared, it is easy to note that *p*-NSF suffers another reduction process (**1c**), E_{p1c} (*p*-NSF) = -0.457 V at 0.04 M BR buffer pH 7.0, which is absent in the *m*-NSF compound, as previously seen in cyclic voltammograms. It is also important to highlight that the reduction process **2c** occurs at less negative potential value than for that observed for the *m*-NSF leader, E_{p2c} (*p*-NSF) = -0.58 V, and E_{p2c} (*m*-NSF) = -0.62 V at 0.04 M BR buffer pH 7.0.

The change in peak potentials (less energy to promote the reduction for *p*-NSF) and the presence of another reduction process (more stable intermediate product), again,

could be associated with the difference in the position of the nitro group in the aromatic structure as can be seen on Scheme 2, which shows a straightforward analogy of the electronic flux involved in the formation of the nitro anion radical ($RNO_2^{\bullet-}$) in the single electron reduction of *p*-NSF and *m*-NSF.

SCHEME 2

As a first step, the single electron reduction of *p*-NSF and *m*-NSF takes place, inducing the homolyses of the π bond between the nitrogen and oxygen present in the nitro moiety, yielding the nitro anion radicals *p*-$NSF^{\bullet-}$ and *m*-$NSF^{\bullet-}$ ($RNO_2^{\bullet-}$) [54]. Structure-wise, *p*-$NSF^{\bullet-}$ possesses the ability to be stabilized by the resonance of the lone pair allocated in the nitrogen, disrupting the aromaticity of the benzenic ring as well as the double bond between the sulfur and oxygen in the sulfonyl portion. Thus, the presence of resonance structures of *p*-$NSF^{\bullet-}$ could considerably escalate its lifetime during the electrochemical measurements.

To evaluate the reversibility of the generated reduction products, square wave voltammograms (SWVs) were obtained at GCE in 0.04 M BR buffer with different values of pH (4.0, 7.0, and 10) containing 1.0 mM *p*-NSF and *m*-NSF and in the absence of oxygen, Figure 5.

FIGURE 5

Data indicate that process **2c** is irreversible at pH 4.0 for *p*-NSF and *m*-NSF, given that the backward current ($I_{backward}$) does not present any anodic components. With the increase in pH value (7.0 and 10), the reversibility of process **2c** appears, with the presence of the anodic component on the backward current, with values of $I_{p,\ forward}/I_{p,\ backward}$ closer to 1 at pH 10 for both compounds. Again, process **1c** is only detected at the measurements conducted for *p*-NSF, and the anodic current component

($I_{backward}$) increases with the increase in the pH of the buffer solution for both **2c** and **1c**. Process **3c** and **4c** do not appear to be reversible in any of the pH range evaluated.

Given the differences in the electrochemical characterization for both compounds, regarding the reduction processes **1c** and **2c**, the evaluation of the reduction pathway aids in gathering information regarding their proposed biological action. Process **2c** can be attributed to the main reduction of the nitro group, according to *(reaction 1)*,

$RNO_2 + 4e^- + 4H^+ \rightarrow RNHOH + H_2O$ *(reaction 1)*

$4.0 < pH < 6.0$

in which, in lower values of pH, the hydroxylamine derivative is formed in a unique step of reduction involving 4 electrons and 4 protons, favored by the availability of protons in the electrolyte solution, E_{p2c} peaks in figures 3A and 4A. The irreversibility of this reduction process was confirmed using square wave voltammetry, E_{p2c} peaks in Figure 5A, and 5D.

On the other hand, the reduction of nitro compounds in intermediate and high values of pH favors the stabilization of the reactive intermediate such as nitro radical anion and nitroso derivative, which significantly slow down further reduction to hydroxylamine, Figure 3B and 5B. Given that the availability of protons decreases, the formation of the nitroso derivative is favored, according to *(reaction 2)*,

$RNO_2 + 2e^- + 2\ H^+ \rightarrow RNO + H_2O$ *(reaction 2)*

$7.0 < pH < 10$

in which two electrons and two protons are involved. The slope of the E_p vs pH for both compounds does not indicate that there is an involvement with protons for this reduction

process. However, the reduction pathway of nitro compounds towards the formation of the nitroso derivative occurs through a cascade reaction, in which there is the formation of the nitro anion radical. Probably, it is possible that the last step of the reduction process is seen, which involves the transfer of one electron from the nitro anion radical to generate the nitroso derivative, in a process which also involves the loss of a water molecule. This hypothesis agrees with the data for $W_{1/2}$ obtained for *p*-NSF.

As previously mentioned, the molecular design of *p*-NSF and *m*-NSF drug leaders aims towards the interference with the parasite metabolism in 3 different ways. The furoxan ring attached to both molecules is unstable in aqueous media, especially in higher values of pH, in which the hydrolysis of the furoxan ring is facilitated and introduces nitric oxide in the cell of the parasite, further inducing apoptosis and cell death [49]. In the electrochemical measurements conducted for both compounds, process **3c** is observed, however, it is not present in the voltammograms of nitrobenzene and *p*-MS, which do not have the furoxan ring in their molecule structure. This process could be associated with the reduction process of a product generated from the hydrolysis of the furoxan ring, in which its magnitude of current increases whenever the pH value of the media increases [55]. Moreover, process **4c** could be attributed to the reduction process of the sulfone moiety, another functional group present in both molecules and introduced to improve membrane permeability within the parasitic cell. Still, given that neither process **3c** nor process **4c** is directly related to the nitro group and also it appears that there is no influence from these processes on the electrochemical direct response of the nitro group reduction, no assumptions were further verified.

Process **1c** occurs at less negative potential values than process **2c** and its occurrence can be associated with the reduction of the nitro group in the formation of its first unstable intermediate, the nitro anion radical, according to *(reaction 3)*,

$RNO_2 + 1e^- \rightarrow RNO_2^{\bullet -}$ *(reaction 3)*

$6.0 < pH < 10$

It is usually difficult to detect the free nitro anion radical at glassy carbon electrodes and in aqueous media, as well as any reactive oxygen or nitrogen species, given its short lifetime and high reactivity [56,57]. Most studies regarding the characterization of the nitro anion radical are performed in organic or aprotic media [58], in which its reversibility is easily seen, or at a boron-doped diamond electrode, where the reduction process is observed whenever a high boron doping content is ensured [35]. In biological systems, the futile cycle of nitro anion radical in the presence of oxygen usually entails competition between the radical's natural decay mechanism and the one-electron transfer to oxygen generating superoxide radicals [17]. Therefore, to further confirm if process **1c** could be correctly attributed to the formation of the nitro radical anion in aqueous media and simulate biological conditions, pulse voltammograms for both compounds were obtained in the presence of oxygen. Moreover, DP voltammograms were also obtained with *p*-NSF in the presence of cysteine, which has been proved to induce the direct reduction of the nitro group towards the nitroso derivative by adduct formation [34]. For both cases, further reduction processes, characteristics of the nitro group reduction, are hindered.

Influence of O_2 and cysteine

DP voltammograms in the presence of oxygen were obtained at GCE in 0.04 M BR buffer pH 7.0 containing 1.0 mM of *p*-NSF and *m*-NSF**.** With the increase in the amount of oxygen inside of the electrochemical cell (bubbling oxygen gas during 10, 20, and 30s) the magnitude of current for process **1c** increases as well, Figures 6A and

6B. This process is unrelated to the oxygen reduction process itself at -0.63 V, as illustrated in Figures S9 and S10.

FIGURE 6

A simple comparison between figures 6A and 6B shows that the process detected at Ep_{1c} is initially present only in the voltammograms obtained in the solutions containing *p*-NSF. It appears in solutions containing *m*-NSF, only after there is the availability of O_2, and, for both cases, the current levels increased with the increase of oxygen amongst the electrochemical cell. These results agree with the hypothesis that process **1c** can be attributed to the formation of the nitro anion radical, according to *(reaction 4)*[35],

$$RNO_2^{\bullet-} + O_2 \rightarrow RNO_2 + O_2^{\bullet-} \qquad \textit{(reaction 4)}$$

in which the intermediate reduction product interacts with oxygen, generates superoxide radicals, and regenerates the initial nitro compound in an electrocatalytic cycle.

DP voltammograms were also obtained at GCE in 0.04 M BR buffer pH 7.0 containing 0.5 mM of *p*-NSF and increasing concentration of cysteine (0.25 mM, 0.5 mM, and 1.0 mM), in the presence of oxygen, Figure 7A, and an absence of oxygen, Figure 7B. The interaction of the nitroso derivative with thiol molecules has already been reported [34,45], in which, in acidic and neutral media and under no applied potential, there is the formation of an adduct between both species, which is further chemically reduced to hydroxylamine derivative, *(reaction 5)*,

$$RNO + 2RSH \rightarrow RNHOH + RS\text{-}SR \qquad \textit{(reaction 5)}$$

There is a depletion in current levels for process **1c** whenever cysteine is present until it is entirely hindered at ratios equal or higher than 1:1 cysteine:*p*-NSF. In the

presence of oxygen, Figure 7B, where the nitro anion radical is easily seen due to the previous electrocatalytic mechanism illustrated, the same depletion is observed, however, the cysteine concentration needed to hinder its current levels completely is higher than 2:1 cysteine:*p*-NSF. This mainly occurs given that oxygen and cysteine have opposite effects over the nitro anion radical production. The adduct formed between the nitroso derivative and thiol molecules may affect the cascade reaction for the generation of the nitro anion radical, destabilizing it (process **1c**), and instead, drives the reduction process under applied potential towards the direct formation of the nitroso derivative. In fact, in square wave voltammograms obtained for *p*-NSF in the absence and presence of cysteine in pH 7.0 and pH 10.0, Figure S11 and S12, respectively, the backward current component for the generation of the nitroso derivative shows a depletion in current values whenever cysteine is present, further confirming the chemical reaction described in *(reaction 5)*. Moreover, the reduction of the nitro compound to hydroxylamine in acid or neutral media containing cysteine is inhibited and the reduction step to the nitroso derivative is favored due to the presence of the coupled chemical reaction.

3.2 Stabilization of $RNO_2^{\bullet-}$ between *p*-NSF and *m*-NSF and comparison with other antichagasic pharmaceuticals

As previously mentioned, the reduction potential of the nitro group can be associated with the degree of injury within the parasite's cell, since less negative potentials are required to generate reactive intermediates such as the nitro anion radical, nitroso derivative, and hydroxylamine. *p*-NSF presents a less negative reduction potential for the nitro group when compared with *m*-NSF, which indicates that this molecular structure, where the nitro group is in *para*- position, is preferred to incite higher biological activity. Moreover, the lower reduction potential and the higher

stability of the nitro anion radical due to a higher number of resonance structures also increase the reactivity of *p*-NSF when compared to *m*-NSF. Table 1 shows a comparison of reduction potential observed in carbon-based electrodes of nitroaromatic compounds in protic media. For these compounds, the generation of the nitro anion radical is often only observed in aprotic or organic media, while the nitro group reduction in aqueous media produces the nitroso derivative or still hydroxylamine. Both compounds, *p*-NSF and, *m*-NSF presents reduction potentials close to pharmaceuticals already used in the treatment of Chagas disease, which, alongside their other structural designed moieties, indicates their potential to be investigated as pharmaceutical antichagasic candidates. The *in vitro* biological experiments to confirm this hypothesis will be performed.

TABLE 1

Thus, the electrochemical characterization of these compounds is particularly important to understand more deeply the mechanism of action of bioactive compounds, as well as to aid in the structural and configuration design of their functional groups in aromatic rings towards the development of new pharmaceutical molecules.

4. CONCLUSIONS

The electrochemical reduction mechanism of two candidates of drug leaders against Chagas disease, *p*-NSF, and *m*-NSF, were investigated in the presence and absence of oxygen using cyclic, differential pulse, and square wave voltammetry. The detection of the nitro anion radical from the reduction processes of the nitro group was evaluated in aqueous media at a bare glassy carbon electrode previously polished and stabilized in a buffer solution. Both compounds presented similar oxidation and reduction processes in the absence of oxygen given their similar molecular structure (reduction to the formation of nitroso derivative in intermediate and higher values of pH and

hydroxylamine in lower values of pH). However, *p*-NSF presented one reduction process that was not observed in the voltammograms for *m*-NSF, **1c**, the generation of the nitro anion radical. The higher stability of this radical intermediate (and an increased lifetime to be registered using voltammetry in aqueous media) was associated with the electronic flux of the *p*-$NSF^{\bullet-}$. This compound presents more resonance structures than *m*-$NSF^{\bullet-}$, hypothesis further confirmed with data obtained using differential pulse voltammetry in the absence and presence of cysteine and oxygen. Cysteine (thiol) forms an adduct with nitroso derivatives, which favors the reduction process in a step involving 2 electrons and 2 protons, even in an acidic medium, where hydroxylamine is normally produced. In the presence of oxygen, the nitro anion radical is consumed to generate superoxide and the original nitro compound, in a catalytic cycle. Therefore, the reduction potential of the nitro group of *p*-NSF, when compared with *m*-NSF, alongside the higher stabilization of the nitro anion radical due to a higher number of resonance structures, indicates that this molecular structure can be chosen for the design of new antichagasic drugs since that inhibit detoxifying enzymes of the parasite, and further aids the beginning steps of the structural design of new antichagasic pharmaceuticals before bioassays in vitro against the parasite.

Acknowledgments

This study was financed in part by the Coordenação de Aperfeiçoamento de Pessoal de Nível Superior - Brasil (CAPES) - Finance Code 001. The authors would like to thank São Paulo Foundation Research (FAPESP) (Project #2012/06240; #2017/02854-8, #2019/10762-1), CNPq (Project #303206/2019-5 and #140828/2016-8).

Credit Author Statement

Caroline G. Sanz: First author and main researcher involved in voltammetric measurements, data analysis, original draft preparation, writing, reviewing and editing.

Kevin A. Dias: Organic synthesis characterization of nitro compounds and draft preparation.

Raphael P. Bacil: Data and paper discussion and draft preparation.

Ricardo A.M. Serafim: Organic synthesis of antichagasic leaders, their characterization and draft preparation.

Leandro A. Helgueira: Supervisor of organic synthesis.

Elizabeth I. Ferreira: Supervisor of organic synthesis of antichagasic leaders draft preparation.

Silvia H.P. Serrano: Corresponding author, main supervisor, data discussion analysis and conceptualization of the article, draft preparation, reviewing and editing.

Declaration of Competing Interest

The authors declare that they have no known competing financial interests or personal relationships that could have appeared to influence the work reported in this paper.

5. References

[1] P.J. Hotez, S. Aksoy, P.J. Brindley, S. Kamhawi, What constitutes a neglected tropical disease?, PLoS Negl. Trop. Dis. 14 (2020) 1–6. doi:10.1371/JOURNAL.PNTD.0008001.

[2] WHO | World Health Organization, (accessed July 15, 2020).

[3] P. Chirac, E. Torreele, Global framework on essential health R&D, Lancet. 367 (2006) 1560–1561. doi:10.1016/S0140-6736(06)68672-8.

[4] B. Pedrique, N. Strub-Wourgaft, C. Some, P. Olliaro, P. Trouiller, N. Ford, B. Pécoul, J.-H. Bradol, The drug and vaccine landscape for neglected diseases (2000-11): a systematic assessmentt, Lancet. 1 (2013) E371–E379. doi:10.1016/S2214-109X(13)70078-0.

[5] P. Hotez, S. Aksoy, PLOS Neglected Tropical Diseases: Ten years of progress in neglected tropical disease control and elimination … More or less, PLoS Negl. Trop. Dis. 11 (2017). doi:10.1371/journal.pntd.0005355.

[6] A. Rassi, A. Rassi, J.A. Marin-Neto, Chagas disease, Lancet. 375 (2010) 1388–1402. doi:10.1016/S0140-6736(10)60061-X.

[7] C. Chao, J.L. Leone, C.A. Vigliano, Chagas disease: Historic perspective, Biochim. Biophys. Acta - Mol. Basis Dis. 1866 (2020). doi:10.1016/j.bbadis.2020.165689.

[8] S. Aldo, C. Valente, H.F. Neto, Considerations on the Epidemiology and Transmission of Chagas Disease in the Brazilian Amazon, Mem. Inst. Oswaldo Cruz. 94 (1999) 395–398.

[9] J.P. Dias, S. Brener, Chagas' disease and blood transfusion, Mem. Inst. Oswaldo Cruz. 79 (1984) 139–147.

[10] R.M. Mills, Chagas Disease: Epidemiology and Barriers to Treatment, Am. J. Med. (2020). doi:10.1016/j.amjmed.2020.05.022.

[11] J.M. Kratz, Drug discovery for chagas disease: A viewpoint, Acta Trop. 198 (2019). doi:10.1016/j.actatropica.2019.105107.

[12] S.S. Santos, R.V. de Araújo, J. Giarolla, O. El Seoud, E.I. Ferreira, Searching for drugs for Chagas disease, leishmaniasis and schistosomiasis: a review, Int. J. Antimicrob. Agents. 55 (2020). doi:10.1016/j.ijantimicag.2020.105906.

[13] A.F. Francisco, S. Jayawardhana, F. Olmo, M.D. Lewis, S.R. Wilkinson, M.C. Taylor, J.M. Kelly, Challenges in Chagas Disease Drug Development, Molecules. 25 (2020). doi:10.3390/molecules25122799.

[14] T. Battista, G. Colotti, A. Ilari, A. Fiorillo, Targeting trypanothione reductase, a key enzyme in the redox trypanosomatid metabolism, to develop new drugs against leishmaniasis and trypanosomiases, Molecules. 25 (2020). doi:10.3390/molecules25081924.

[15] K. Vázquez, M. Paulino, C.O. Salas, J.J. Zarate-Ramos, B. Vera, G. Rivera, Trypanothione Reductase: A Target for the Development of Anti- Trypanosoma cruzi Drugs, Mini-Reviews Med. Chem. 17 (2017). doi:10.2174/1389557517666170315145410.

[16] F.R. Paula, S.H.P. Serrano, L.C. Tavares, Aspectos mecanísticos da bioatividade e toxicidade de nitrocompostos, Quim. Nova. 32 (2009) 1013–1020.

[17] P. Wardman, Some Reactions and Properties of Nitro Radical-Anions Important in Biology and Medicine, Environ. Health Perspect. 64 (1985) 309. doi:10.2307/3430019.

[18] A. Zahoor, M.V.M.M. Lafleur, R.C. Knight, H. Loman, D.I. Edwards, DNA damage induced by reduced nitroimidazole drugs, Biochem. Pharmacol. 36 (1987) 3299–3304. doi:10.1016/0006-2952(87)90648-4.

[19] G.E. Adams, E.D. Clarke, R.S. Jacobs, I.J. Stratford, R.G. Wallace, P. Wardman, M.E. Watts, Mammalian cell toxicity of nitro compounds: Dependence upon reduction potentiakl, Biochem. Biophys. Res. Commun. 72 (1976) 824–829. doi:10.1016/S0006-291X(76)80207-0.

[20] F.C. de Abreu, P.A. de L. Ferraz, M.O.F. Goulart, Some Applications of Electrochemistry in Biomedical Chemistry. Emphasis on the Correlation of Electrochemical and Bioactive Properties, J. Braz. Chem. Soc. 13 (2002) 19–35. doi:10.1590/S0103-50532002000100004.

[21] G. Dryhurst, Electrochemistry of biological molecules, Academic Press, 1977.

[22] S. Bollo, L.J. Núñez-Vergara, C. Martinez, G. Chauviere, J. Périé, J.A. Squella, Voltammetric study of nitro radical anion generated from some nitrofuran compounds of pharmacological significance, Electroanalysis. 15 (2003) 19–25. doi:10.1002/elan.200390000.

[23] L.D. Chiavassa, M.A. La-Scalea, Square wave voltammetry of nitrofurans in aqueous media using a carbon fiber microelectrode, J. Solid State Electrochem. 22 (2018) 1395–1402. doi:10.1007/s10008-017-3751-8.

[24] J. Stradins, R. Gavars, L. Baumane, Intermediate products of electrochemical reduction of nitrofurans in aprotic media, Electrochim. Acta. 28 (1983) 495–500. doi:10.1016/0013-4686(83)85033-6.

[25] J.A. Squella, M.E. Letelier, L. Lindermeyer, L.J. Nuñez-Vergara, Redox behaviour of nifuroxazide: Generation of the one-electron reduction product, Chem. Biol. Interact. 99 (1996) 227–238. doi:10.1016/0009-2797(95)03672-5.

[26] C. Yañez, J. Pezoa, M. Rodríguez, L.J. Núñez-Vergara, J.A. Squella, Voltammetric Behavior of a 4-Nitroimidazole Derivative, J. Electrochem. Soc. 152 (2005) J46. doi:10.1149/1.1904983.

[27] J.A. Squella, A. Campero, J. Maraver, J. Carbajo, Electrochemical reduction of 2-nitroimidazole in aprotic medium : Influence of its dissociation equilibrium on the reduction mechanism, 52 (2006) 511–518. doi:10.1016/j.electacta.2006.05.032.

[28] A.M.O. Brett, S.H.P. Serrano, I. Gutz, M.A. La-Scalea, M.L. Cruz, Voltammetric Behavior of Nitroimidazoles at a DNA-Biosensor, Electroanalysis. 9 (1997) 1132–1137. doi:10.1002/elan.1140091419.

[29] J.A. Squella, L.J. Núñez-Vergara, A. Campero, J. Maraver, P. Jara-Ulloa, J. Carbajo, Electrochemical Reduction of 2-Nitroimidazole in Aqueous Mixed Medium, J. Electrochem. Soc. 154 (2007) F77. doi:10.1149/1.2472553.

[30] J.H. Tocher, Reductive activation of nitroheterocyclic compounds, Gen. Pharmacol. 28 (1997) 485–487. doi:10.1016/S0306-3623(96)00283-2.

[31] L.J. Núñez-Vergara, M.E. Ortiz, S. Bollo, J.A. Squella, Electrochemical generation and reactivity of free radical redox intermediates from ortho-and meta-nitro substituted 1,4-dihydropyridines, Chem. Biol. Interact. 106 (1997) 1–14. doi:10.1016/S0009-2797(97)00050-1.

[32] M.A. La-Scalea, S.H.P. Serrano, I.G.R. Gutz, Voltammetric Behaviour of Metronidazole at Mercury Electrodes, J. Braz. Chem. Soc. 10 (1999) 127–135. doi:10.1590/S0103-50531999000200010.

[33] M.A. La-Scalea, G.H.G. Trossini, C.M.S. Menezes, M.C. Chung, E.I. Ferreira, Electrochemical Reduction Using Glassy Carbon Electrode in Aqueous Medium of a Potential Anti-Chagas Drug: NFOH, J. Electrochem. Soc. 156 (2009) F93. doi:10.1149/1.3130082.

[34] M.S. d. S. Julião, E.I. Ferreira, N.G. Ferreira, S.H.P. Serrano, Voltammetric detection of the interactions between $RNO_2^{\bullet-}$ and electron acceptors in aqueous medium at highly boron doped diamond electrode (HBDDE), Electrochim. Acta. 51 (2006) 5080–5086. doi:10.1016/j.electacta.2006.03.054.

[35] M.S. da S. Julião, É.C. Almeida, M.A. La Scalea, N.G. Ferreira, R.G. Compton, S.H.P. Serrano, Voltammetric behavior of nitrofurazone at highly boron doped diamond electrode, Electroanalysis. 17 (2005) 269–274.

[36] D.C. Tiwari, R. Jain, S. Sharma, Electrochemically deposited polyaniline/polypyrrole polymer film modified electrodes for determination of furazolidone drug, J. Sci. Ind. Res. (India). 66 (2007). http://nopr.niscair.res.in/handle/123456789/1347 (accessed February 15, 2020).

[37] I. Murueva, J. Romero, C. Espinosa-bustos, electrochemical studies of new 5- and 6-nitro N -acyl-1 H -indazoles, (2011). doi:10.1002/poc.1843.

[38] C. Olea-Azar, C. Rigol, F. Mendizabal, H. Cerecetto, R. Maio, M. Gonzalez, W. Porcal, A. Morello, Y. Repetto, J. Maya, Novel Benzo[1,2-c]1,2,5-Oxadiazole N-Oxide Derivatives as Antichagasic Agents: Chemical and Biological Studies, Lett. Drug Des. Discov. 2 (2005) 294–301. doi:10.2174/1570180054038341.

[39] U.A. Boelsterli, H.K. Ho, S. Zhou, K.Y. Leow, Bioactivation and Hepatotoxicity of Nitroaromatic Drugs, (2006) 715–727.

[40] H. Cerecetto, B. Mester, S. Onetto, G. Seoane, M. González, F. Zinola, Formal potentials of new analogues of nifurtimox: relationship to activity., Farmaco. 47 (1992) 1207–13. http://www.ncbi.nlm.nih.gov/pubmed/1300126 (accessed February 15, 2020).

[41] L.J. Núñez-Vergara, F. García, M.M. Domínguez, J. de la Fuente, J.A. Squella, In situ reactivity of the electrochemically generated nitro radical anion from nitrendipine with glutathione, adenine and uracil, J. Electroanal. Chem. 381 (1995) 215–219. doi:10.1016/0022-0728(94)03647-L.

[42] J.H. Tocher, D.I. Edwards, Evidence for the direct interaction of reduced metronidazole derivatives with DNA bases, Biochem. Pharmacol. 48 (1994) 1089–1094. doi:10.1016/0006-2952(94)90144-9.

[43] X. Jiang, X. Lin, Voltammetry of the interaction of metronidazole with DNA and its analytical applications, Bioelectrochemistry. 68 (2006) 206–212. doi:10.1016/j.bioelechem.2005.08.003.

[44] M. Catalán, A. Álvarez-Lueje, S. Bollo, Electrochemistry of interaction of 2-(2-nitrophenyl)-benzimidazole derivatives with DNA, Bioelectrochemistry. 79 (2010) 162–167. doi:10.1016/j.bioelechem.2010.02.002.

[45] T. Andres, L. Eckmann, D.K. Smith, Voltammetry of nitrobenzene with cysteine and other acids in DMSO. Implications for the biological reactivity of reduced nitroaromatics with thiols, Electrochim. Acta. 92 (2013) 257–268. doi:10.1016/j.electacta.2013.01.047.

[46] P. Nandy, S. Das, Inorganica Chimica Acta In situ reactivity of electrochemically generated nitro radical anion on Ornidazole and its monomeric Cu (II) complex with nucleic acid bases and calf thymus DNA, Inorganica Chim. Acta. 501 (2020) 119267. doi:10.1016/j.ica.2019.119267.

[47] A.M. Oliveira Brett, S.H.P. Serrano, I. Gutz, M.A. La-Scalea, Electrochemical reduction of metronidazole at a DNA-modified glassy carbon electrode, in: Bioelectrochemistry Bioenerg., Elsevier Science S.A., 1997: pp. 175–178. doi:10.1016/S0302-4598(96)05122-7.

[48] M.A. La-Scalea, S.H.P. Serrano, E.I. Ferreira, A.M. Oliveira Brett, Voltammetric behavior of benznidazole at a DNA-electrochemical biosensor, J. Pharm. Biomed. Anal. 29 (2002) 561–568. doi:10.1016/S0731-7085(02)00081-X.

[49] R.A. Massarico Serafim, J.E. Gonçalves, F.P. De Souza, A.P. De Melo Loureiro, S. Storpirtis, R. Krogh, A.D. Andricopulo, L.C. Dias, E.I. Ferreira, Design, synthesis and biological evaluation of hybrid bioisoster derivatives of N-acylhydrazone and furoxan groups with potential and selective anti-Trypanosoma cruzi activity, Eur. J. Med. Chem. 82 (2014) 418–425. doi:10.1016/j.ejmech.2014.05.077.

[50] N.D. Segretti, R.A.M. Serafim, M.C.F. Segretti, M. Miyata, F.R. Coelho, O. Augusto, E.I. Ferreira, New antibacterial agents: Hybrid bioisoster derivatives as potential E. coli FabH inhibitors, 2016.

[51] R. Fruttero, B. Ferrarotti, A. Serafino, A. Di Stilo, A. Gasco, Unsymmetrically substituted furoxans. Part 11 . Methylfuroxancarbaldehydes, J. Heterocycl. Chem. 26 (1989) 1345–1347. doi:10.1002/jhet.5570260523.

[52] W.W. Schoeller, J. Niemann, P. Rademacher, On the electrochemical oxidation of enamines, J. Chem. Soc. Perkin Trans. 2. (1988) 369–373. doi:10.1039/P29880000369.

[53] C. Brett, A. Brett, Electrochemistry: principles, methods, and applications, Springer. (1993) 427.

[54] A. Kuhn, K.G. Eschwege, J. Conradie, Reduction potentials of para-substituted nitrobenzenes-an infrared, nuclear magnetic resonance, and density functional theory study, J. Phys. Org. Chem. 25 (2012) 58–68. doi:10.1002/poc.1868.

[55] M.D. Bartberger, W. Liu, E. Ford, K.M. Miranda, C. Switzer, J.M. Fukuto, P.J. Farmer, D.A. Wink, K.N. Houk, The reduction potential of nitric oxide (NO) and its importance to NO biochemistry, PNAS, 2002. www.pnas.orgcgidoi10.1073pnas.162095599 (accessed October 19, 2019).

[56] A. René, M.L. Abasq, D. Hauchard, P. Hapiot, How do phenolic compounds react toward superoxide ion? A simple electrochemical method for evaluating antioxidant capacity, Anal. Chem. 82 (2010) 8703–8710. doi:10.1021/ac101854w.

[57] C.P. Andrieux, P. Hapiot, J. michel Saveant, Mechanism of Superoxide Ion Disproportionation in Aprotic Solvents, J. Am. Chem. Soc. 109 (1987) 3768–3775. doi:10.1021/ja00246a040.

[58] J. Squella, S. Bollo, L. Nunez-Vergara, Recent Developments in the Electrochemistry of Some Nitro Compounds of Biological Significance, Curr. Org. Chem. 9 (2005) 565–581. doi:10.2174/1385272053544380.

[59] P.C. Mandal, Reactions of the nitro radical anion of metronidazole in aqueous and mixed solvent: A cyclic voltammetric study, J. Electroanal. Chem. 570 (2004) 55–61. doi:10.1016/j.jelechem.2004.02.030.

TABLE OF CONTENTS

TABLE 1

Table 1. Reduction potential and molecular structures of pharmaceuticals against chagas disease.

	Compounds	Reduction potential	Media	Reference
Nitroimidazol derivatives 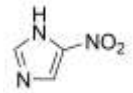	Benznidazol	-0,495 V	0.4 M BR buffer pH 7.5	[48]
	Metronidazol	-0,834 V	50% Aqueous DMF	[59]
		-0,708 V	1 mM citrate buffer pH 7.4	
Nitrofuran derivatives 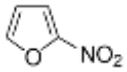	Nitrofurazone	-0.473 V	0.4 M BR buffer pH 9.2	[23]
	Nitrofurantoin	-0.410 V		
	Furazolidone	-0.473 V		
	Nifurtimox	-0.320 V	30/70 ethanol/BR buffer pH 7.0 (KCl 0.3 M)	[22]
Nitrobenzene derivatives 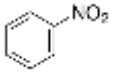	*p*-NSF	-0.58 V	0.04 M BR buffer pH 7.0	This work
	m-NSF	-0.62 V		

FIGURE 1

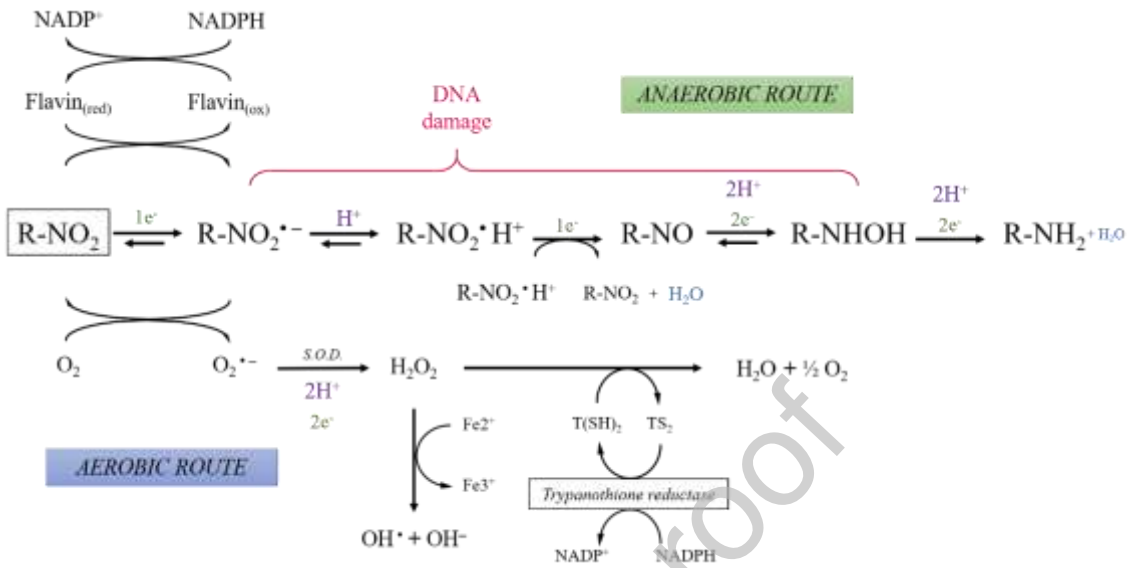

Figure 1. Mechanism of bioreduction of nitrocompounds and their reactive intermediates. Adapted from [16].

FIGURE 2

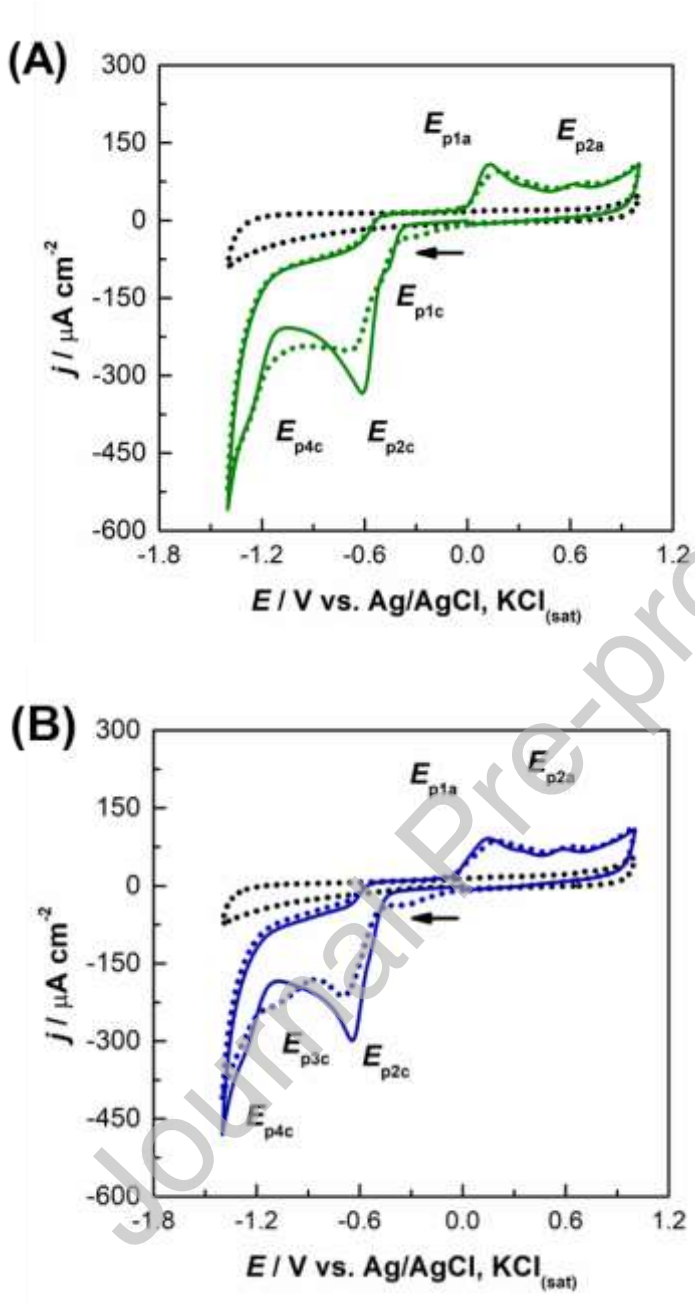

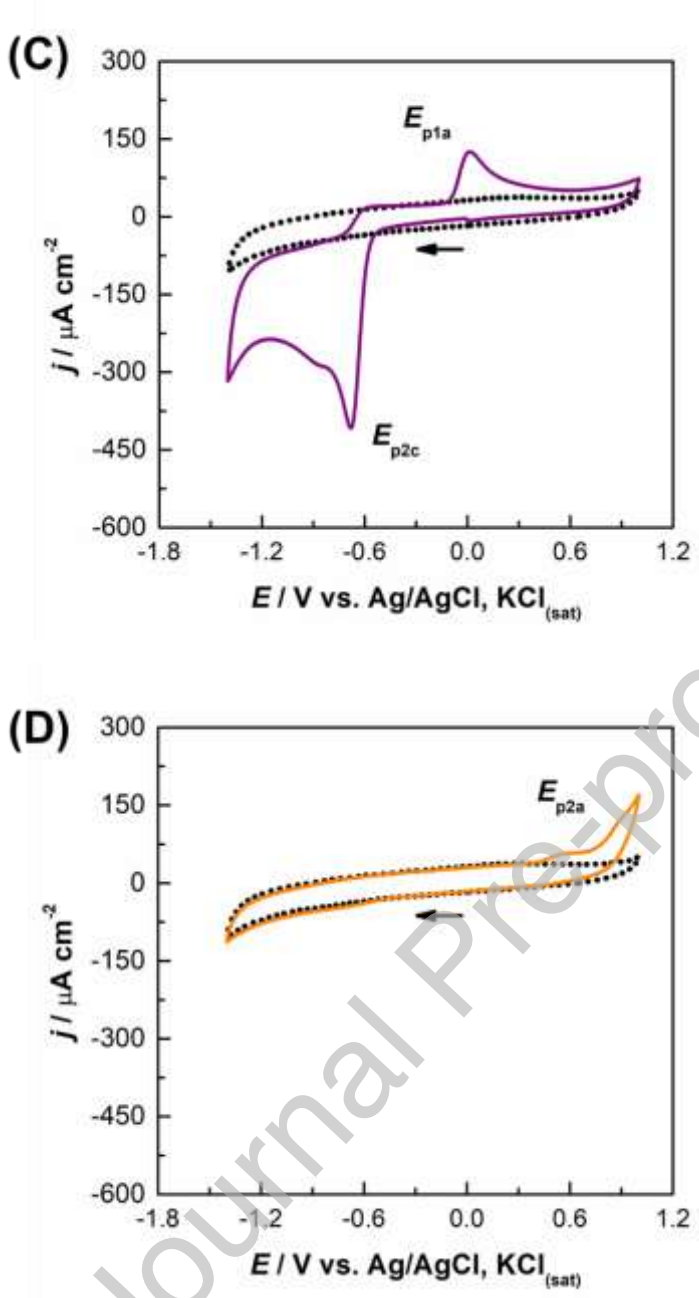

Figure 2. Cyclic voltammograms obtained at GCE in 0.04 M BR buffer pH 7.0 containing 1.0 mM of *p*-NSF (A), 1.0 mM of *m*-NSF (B), 1.0 mM of nitrobenzene (C) and 1.0 mM of *p*-MS (D), in the absence of oxygen. ν = 100 mV s^{-1}, blank (●●●), 1st cycle (solid line ▬, ▬, ▬, ▬) and 2nd cycle (dotted line •••, •••).

FIGURE 3

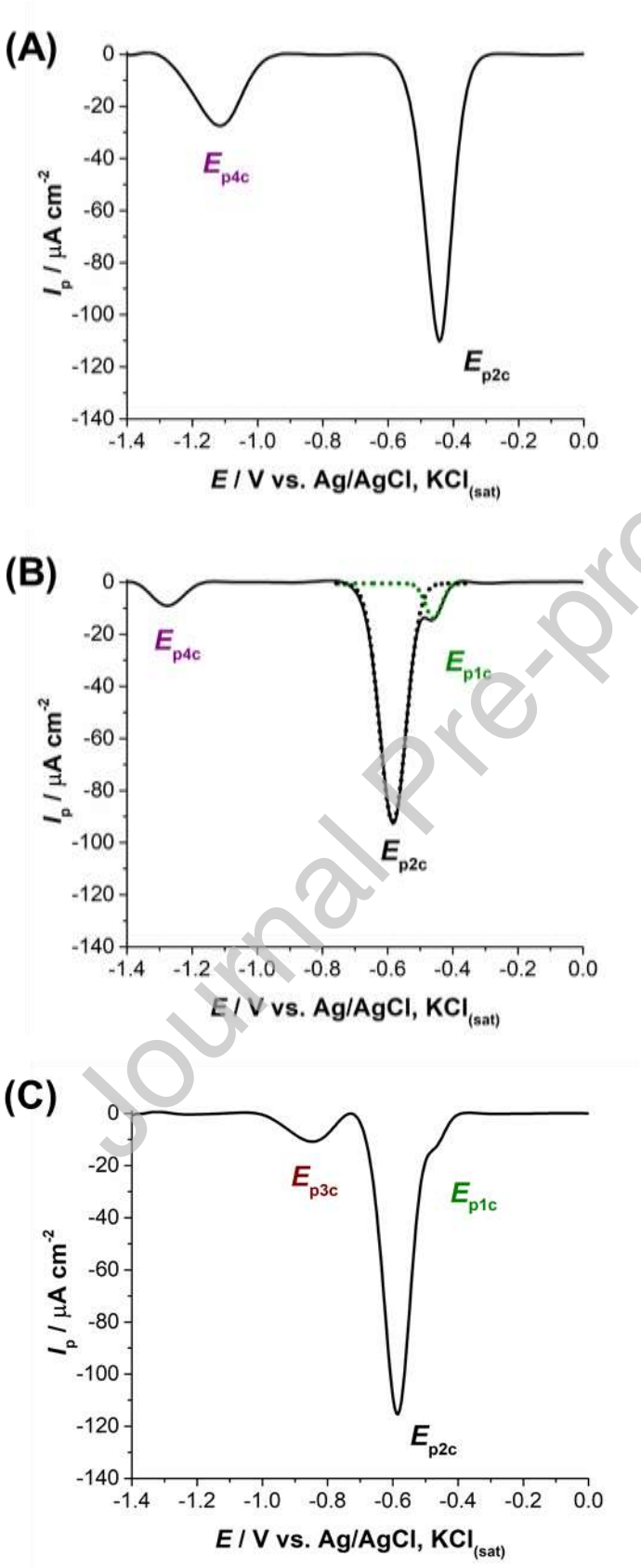

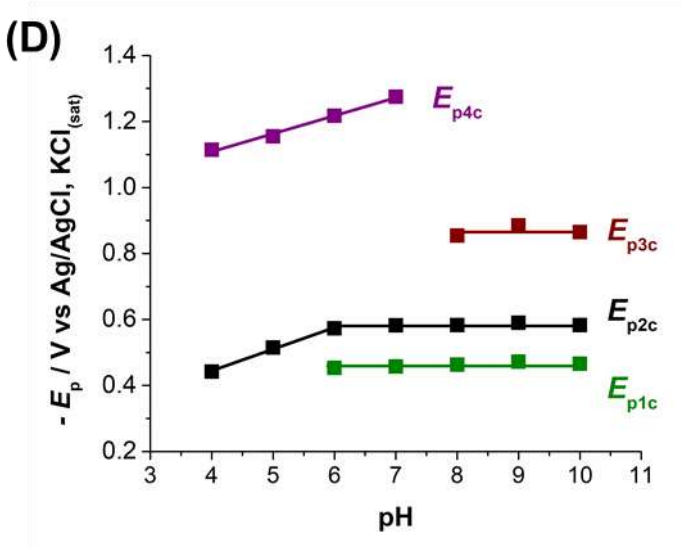

Figure 3. Differential pulse voltammograms at GCE in 0.04 M BR buffer pH 4.0 (A), 7.0 (B), and 10 (C) containing 1 mM of *p*-NSF in the absence of oxygen. E_p vs. pH plots obtained from the respective voltammograms (D).

FIGURE 4

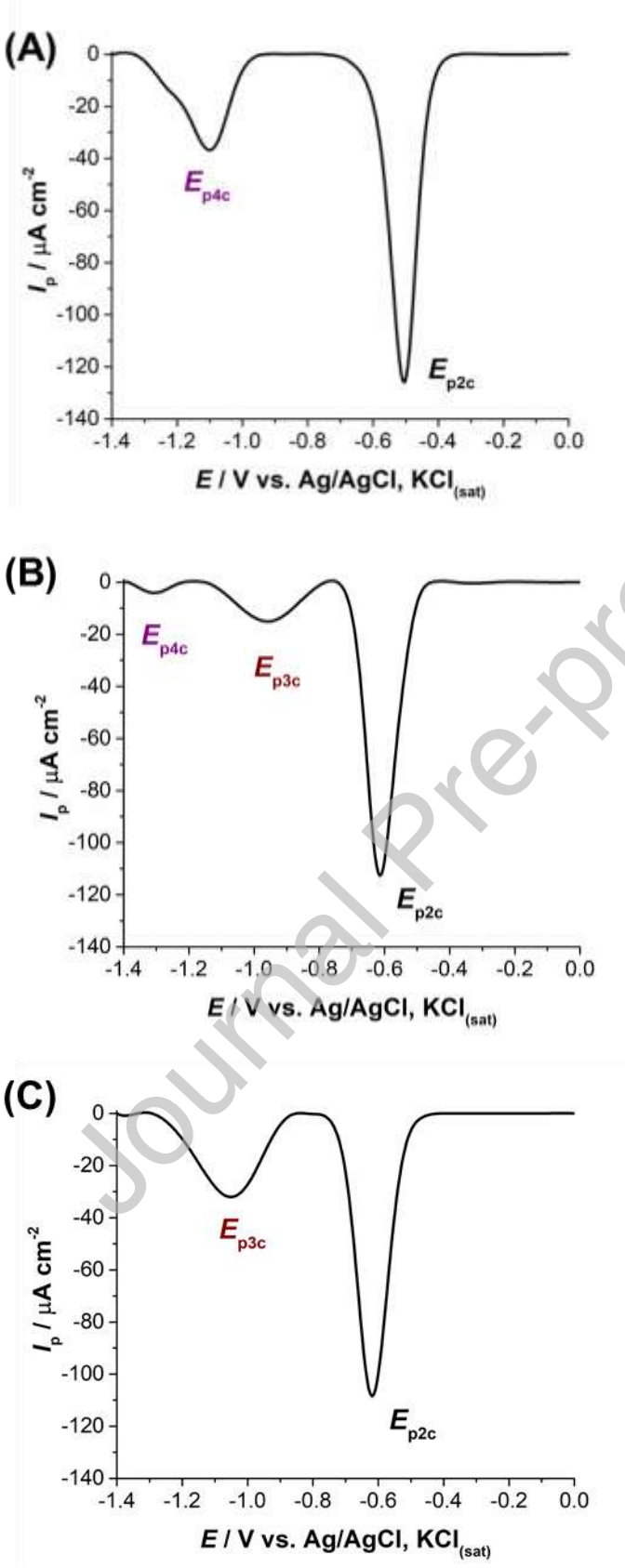

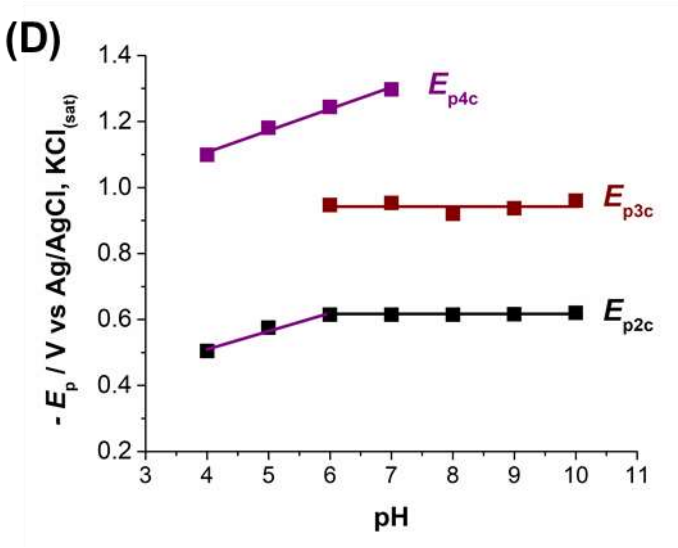

Figure 4. Differential pulse voltammograms at GCE in 0.04 M BR buffer pH 4.0 (A), 7.0 (B) and, 10 (C) containing 1 mM of *m*-NSF in the absence of oxygen. E_p vs. pH plots obtained from the respective voltammograms (D).

FIGURE 5

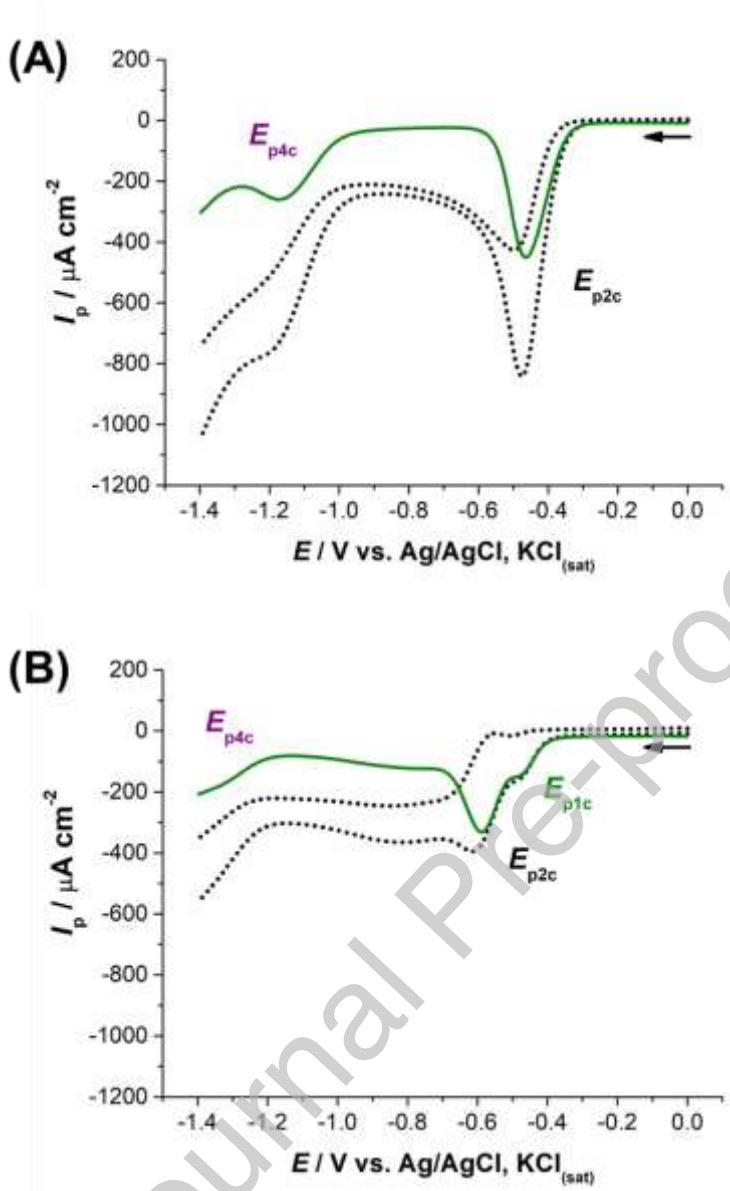

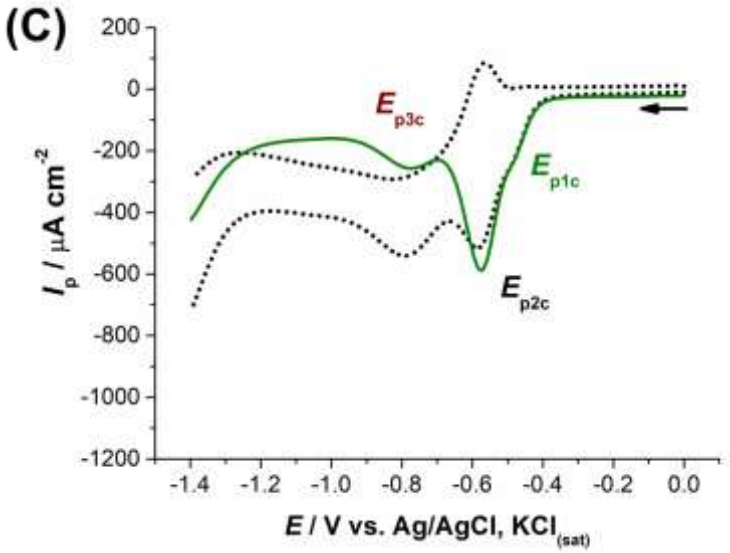

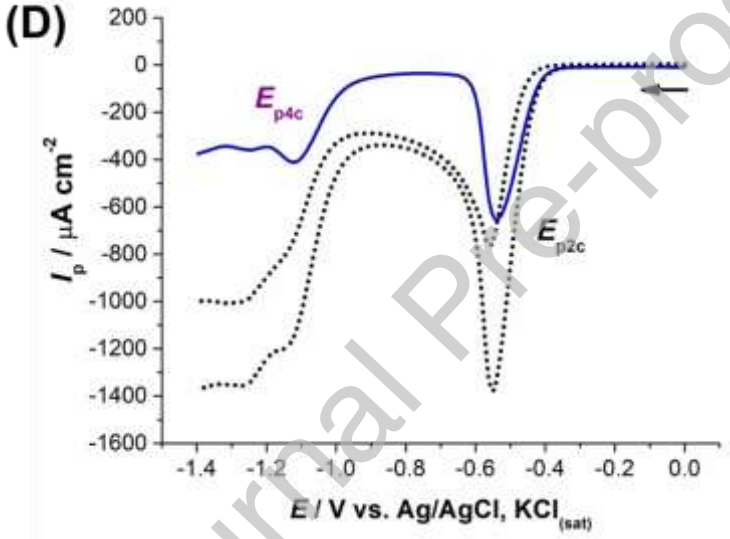

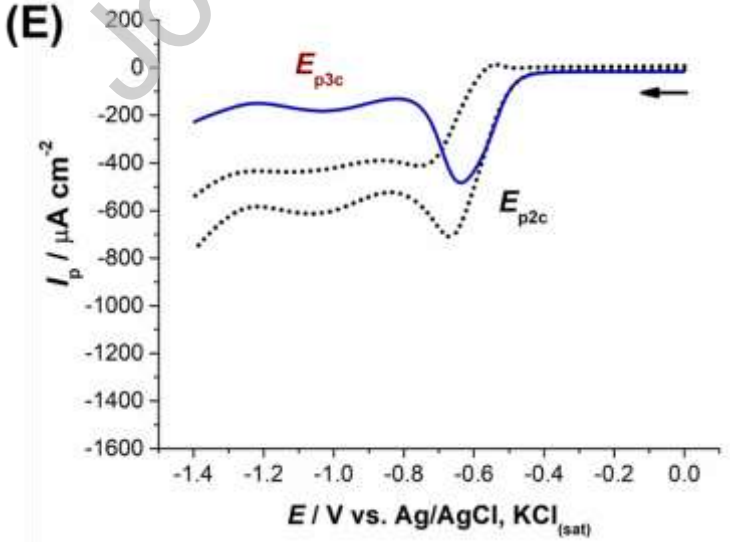

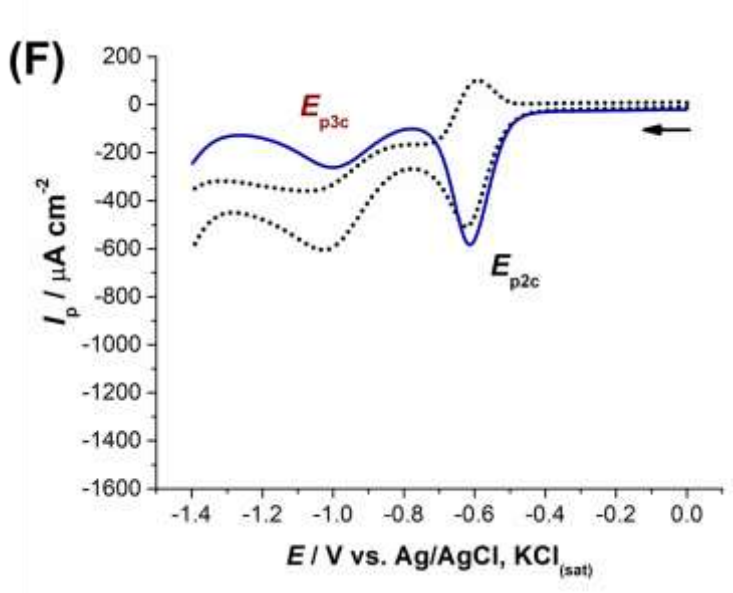

Figure 5. SW voltammograms at GCE in 0.04 M BR buffer pH 4.0 (A,D), 7.0 (B,E) and 10 (C,F) containing 1.0 mM of *p*-NSF (A,B, and C) and 1.0 mM of *m*-NSF (D, E and F) in the absence of oxygen.

FIGURE 6

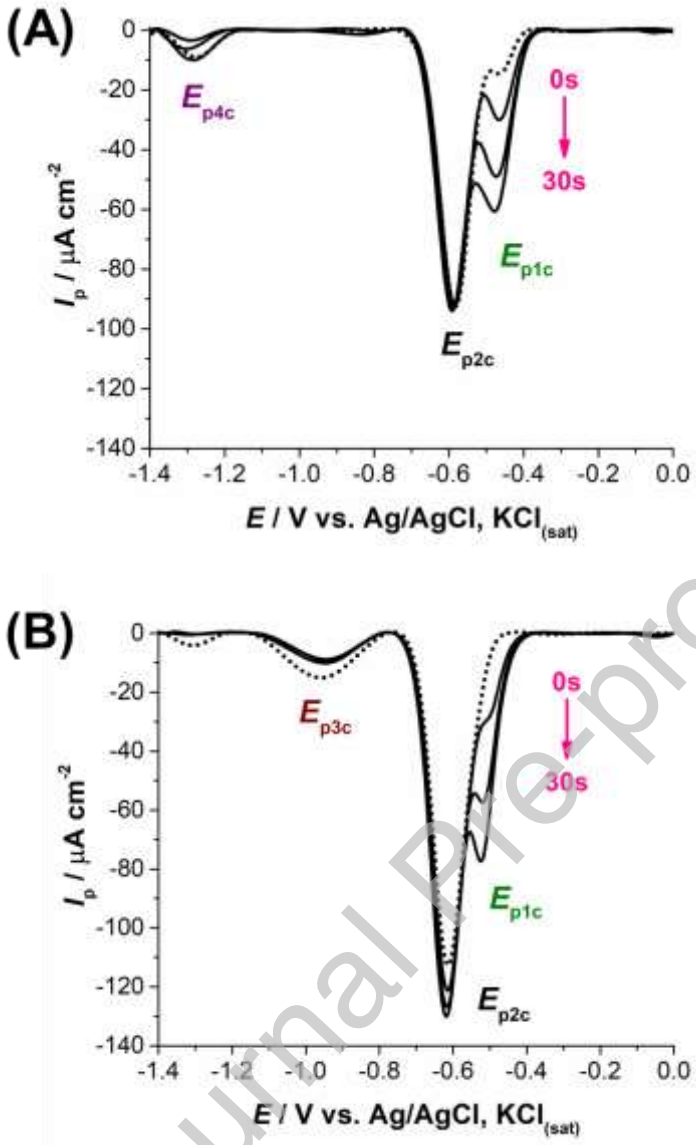

Figure 6. Differential pulse voltammograms at GCE in 0.04 M BR containing 1.0 mM of *p*-NSF (A) and 1.0 mM of *m*-NSF (B) in the absence (•••) and presence (▬) of oxygen with increasing time of O_2 bubbling.

FIGURE 7

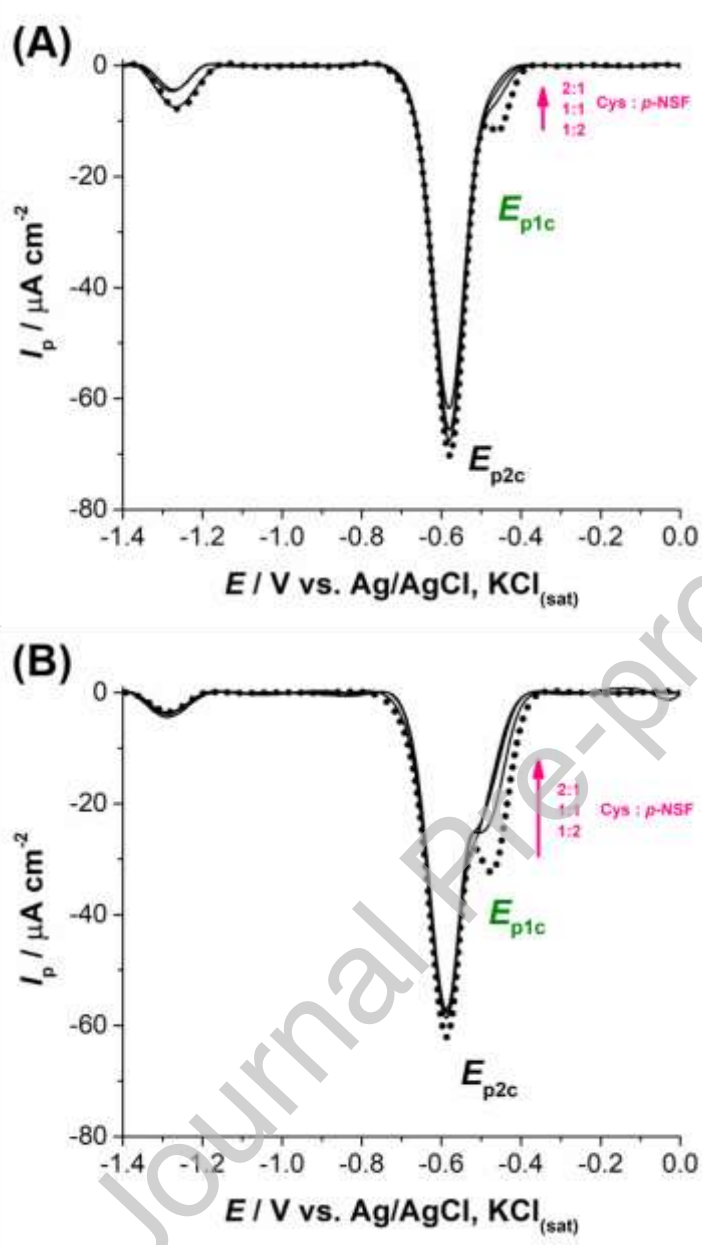

Figure 7. Differential pulse voltammograms at GCE in 0.04 M BR in the presence (A) and absence (B) of O_2, containing 0.5 mM of *p*-NSF (•••), 1:2, 1:1 and 2:1 ratio cysteine:*p*-NSF (▬).

SCHEME 1

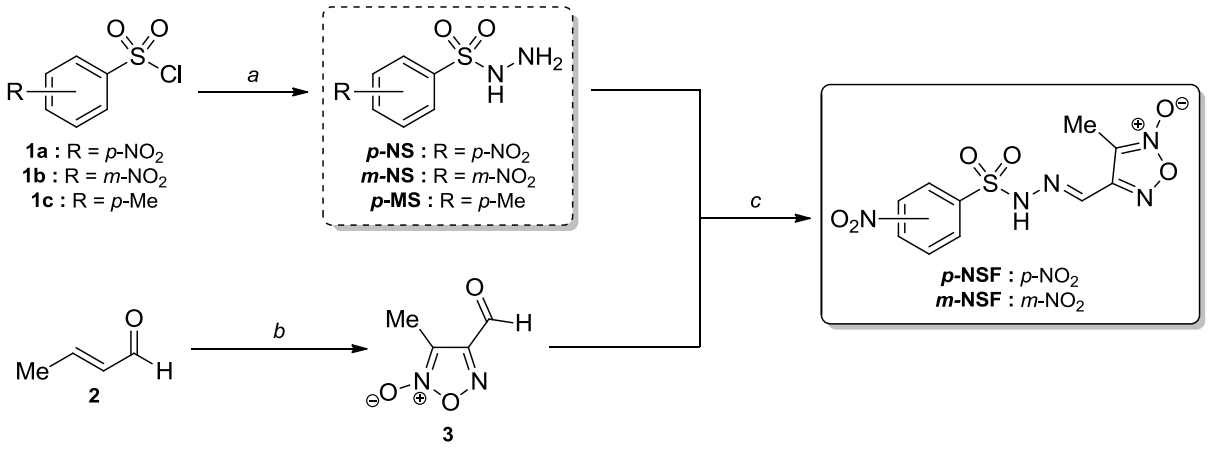

Scheme 1. The convergent synthetic route towards antichagasic leaders *p*-NSF and *m*-NSF. Reaction conditions: hydrazine hydrate 80%, THF, 0 °C, 2-3 h (*step a*), $NaNO_{2(aq)}$, AcOH, 14 °C, 1 h (*step b*) and MeOH, HCl/reflux (*step c*).

SCHEME 2

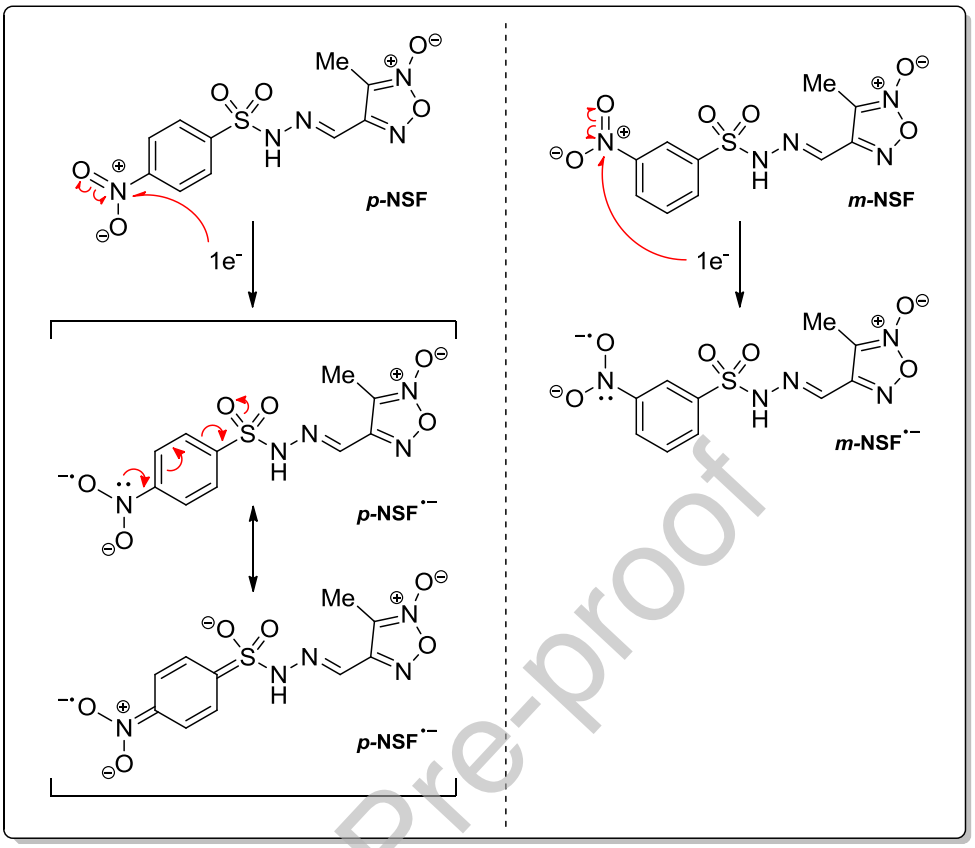

Scheme 2. Resonance structures of the nitro anion radical formed under applied potential by the single electron reduction of *p*-NSF and *m*-NSF.

Graphical Abstract